BEHAVIOUR OF TRANSIENT 2-D LIQUID SHEETS

M. S. Goodwin & G. Wigley

Aeronautical & Automotive Engineering Department, Loughborough University, Loughborough, Leicestershire, LE11 3TU, England.

The mechanisms of liquid break-up have been investigated by many researchers, however, most have concentrated on steady state low pressure conditions. The spray structure produced by high pressure GDI injectors generally consists of a complex hollow cone spray and is transient in nature due to the cyclic behaviour of an SI engine. To allow a simplified analysis of such a spray a rotary slit valve of 20 x 1mm has been designed to produce a transient flat liquid sheet. Operating with the same fuel delivery pressures as GDI injectors the long term view is to conduct a detailed comparison between transient flat and conical liquid sheets. The current work has focused on the pressure range from 10-50 bar. The behaviour of a transient two dimensional liquid sheet is described using CCD macro-imaging, Particle Image Velocimetry, PIV, and Laser Doppler Anemometry, LDA. Development of perforations which in part lead to disintegration have been assessed from a detailed analysis of the CCD images. The propagation of surface waves and structures downstream from the nozzle as a function of time have been measured by a modified PIV technique. The local velocities of the intact liquid sheet, the remnants of the sheet after break-up and droplets due to atomisation at various axial positions downstream from the nozzle slit have been measured using LDA to provide the time averaged histories of the liquid velocity.

1. INTRODUCTION

With increasingly stringent emissions legalisation for road vehicles, the development of more efficient SI engines is important for their long term viability. Gasoline Direct Injection, GDI, offers improved fuel efficiency, and power improvements, with the potential of reduced emissions. Optimisation of this technology and hence compliance with future legalisation will ensure SI engine production into the future. Much work is required to optimise the GDI operating strategies as regards emissions, with the fuel injection process at the centre of the problem.

The GDI fuel injection process is highly complex, with many manufacturers adopting the use of pressure-swirl sprays operating at injection pressures above 50bar [1, 2]. Understanding the behaviour and fuel break-up process of such sprays in a complex engine environment will greatly assist in the development of GDI engine technology. Many fundamental studies [3, 4, 5] have investigated the liquid break-up mechanisms, however, most have studied idealised 2-D steady flow sprays at significantly lower injection pressures to those encountered with GDI sprays. The spray produced by a GDI injector is highly transient, due to the cyclic behaviour of an SI engine, with maximum injection times of up to 5ms.

To simplify the ability to analyse a typical GDI spray while maintaining the transient characteristics, an analysis of a 2-D transient liquid sheet has been undertaken. A unique rotary valve has been specifically designed and manufactured to produce a transient flat liquid sheet under injection pressures of 10-50 bar. The use of various nozzles allowed the analysis of both parallel and divergent liquid sheets to assess the affect of sheet stretching also encountered in a pressure-swirl spray. The behaviour of the transient liquid sheets is described using CCD macro-imaging, Particle Image Velocimetry, PIV, and Laser Doppler Anemometry, LDA.

2. EXPERIMENTAL SETUP

A high pressure fuel injection rig designed around a high pressure Bosch GDI pump with the capability of fuel line pressures of up to 120 bar was used for the study. An adjustable pressure relief valve was used to attain stable fuel line pressures in the range 3-65 bar.

A rotary valve was designed to produce a flat liquid sheet, Figure 1, consisting of a rotating aluminium bronze cylinder (1) inside a stationary stainless steel cylindrical housing (2). The use of these materials minimised friction between the moving parts which were precision ground to provide a close running fit of only 4μm clearance around the circumference to minimise fuel leakage. Both (1) and (2) have a single spark eroded slot in the cylindrical walls on a plane through their diameters. Unleaded gasoline was used for the investigation, entering the cylinder chamber from one end of the rotating assembly and emitted through the 1 x 20mm slot when aligned with the 1 x 30mm slot in the housing. The expansion in the slot length was designed to absorb any pressure fluctuations inherent of the system. A

1.7Nm AC brushless motor was used to drive the rotary valve through a 10:1 gearbox, providing 16Nm continuous and 30Nm peak torque. The servo drive was programmed to rotate the cylinder once, at a speed of 150rpm, providing an injection duration of 5.1ms. Three interchangeable brass nozzles (3), parallel, 20° and 30° divergence, thin the sheet from 1mm to 0.15mm whilst expanding the sheet laterally, with a minimum aspect ratio of 200:1.

An optical encoder located on the drive shaft provided one TTL pulse per revolution, to trigger two CCD cameras and the strobes simultaneously. To study the liquid sheet a PCO fast shutter SensiCam SuperVGA 12 bit camera was used with a Nikon 55mm focal length macro lens to provide an image size of 100 by 60mm represented by 1280 by 1024 pixels. An EG&G MVS 7020 Xenon flash unit linked to a Fostec fibre optic panel was positioned behind the spray to provide uniform back-lighting. The use of two cameras allowed front and side imaging of the flat liquid sheet. The TTL pulse was positioned as close to the opening point as possible to minimise any cycle to cycle variations. A signal delay unit was then used to increment the image capture time allowing an assessment of the temporal sheet development.

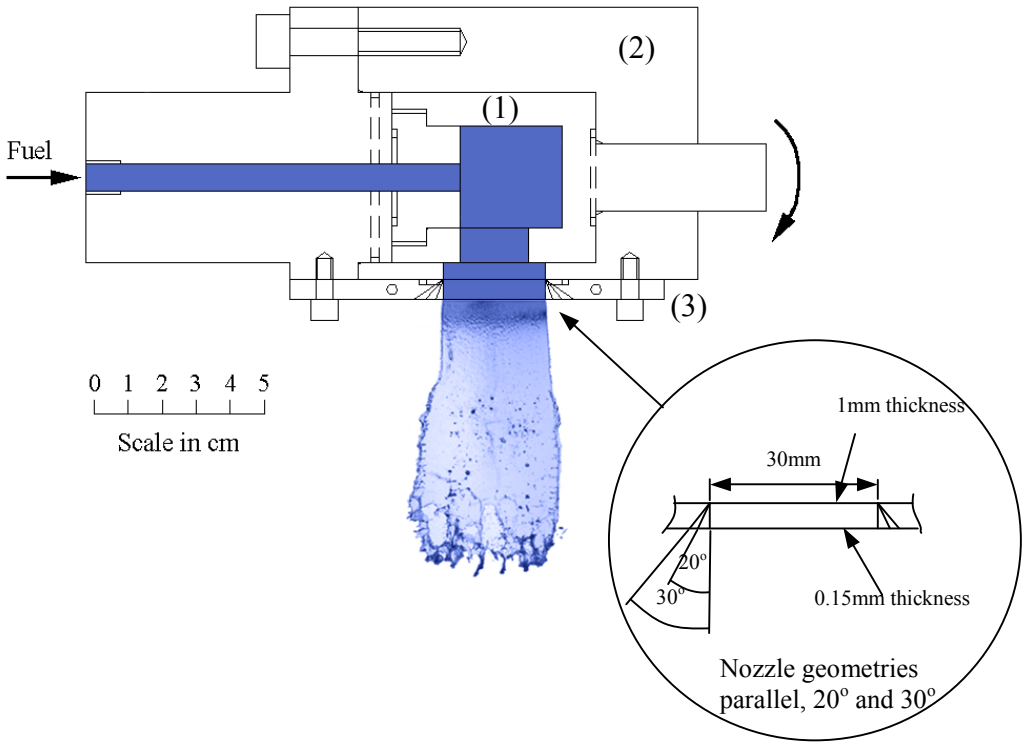

Figure 1. Rotary valve design and three nozzle configurations

Quantitative spray information was obtained using Particle Image Velocimetry, PIV and Laser Doppler Anemometry, LDA. A cross-correlation PIV method was adopted for this study to further aid the analysis of the flat liquid sheet. Rather than seeding the flow with particles, surface structures in the form of waves and perforations were tracked between images. This technique was also adopted by Broll and Walzel [6] to assess the flow field produced by a pressure swirl spray operating between 0.5 and 1.6 bar injection pressure. In their investigation an LED panel was positioned behind the spray and a 105mm lens was used to allow near nozzle imaging.

For this study a 120mJ laser was positioned behind the liquid sheet in conjunction with a divergent lens and a fluorescing 'gel' panel to provide uniform back illumination. The system was arranged to capture two 7ns exposures by pulsing the laser with a temporal separation of 20μs, providing a pixel movement range of 3 – 9 based on a velocity range of 12 – 36m/s respectively.

The temporal sheet development was investigated using all three nozzles at three injection pressures of 10, 20 and 30 bar. At each test condition, 10 double exposure images were captured in succession to allow an average flow field to be calculated. A batch processing technique was adopted whereby each image pair was subjected to 5 correlations of progressively decreasing interrogation window size, 256 x 256, 128 x 128, 64 x 64, 32 x 32, and 32 x 32 pixels. An average vector field was then calculated from the batch.

The two component LDA system used laser wavelengths of 488 and 514nm and powers of 120 and 250mW respectively [7]. Each beam was split into two coherent parallel beams using a Bragg cell and beam expanding optics and focused by the final lens to form two coincident measurement volumes of 42 and 45μm diameters. The optical receiver, Dantec 57X10, was positioned at a 70 degree scattering angle and a 0.5mm aperture was used producing a measurement volume of 0.1mm in length.

With an injection timing of 1Hz the acquisition software was configured to collect 10,000 velocity samples over a maximum period of 100 seconds. The LDA measurement volume was positioned in the centre of the liquid sheet, to avoid edge effects, and on the nozzle axis to locate the zero position. Once the zero position was located, radial scans were undertaken using a precision traverse with a digital vernier to accurately position the rotary valve, and liquid sheet, relative to the measurement volume. Radial scans were conducted at 6 locations down the sheet axis, 10, 20, 30, 50, 75

and 100mm. In the near nozzle region scans were initiated 5mm off-axis and then incremented, in 0.25mm steps, towards the spray axis, whereas, further downstream scans were started 7mm off-axis with 0.5mm increments.

3. DISCUSSION OF RESULTS

The spray imaging allowed a detailed assessment of the behaviour of the transient liquid sheet and its break-up mechanism [8, 9]. It was possible to quantify the transient sheet penetration over the injection pressure range 10 – 50 bar and the development of perforations in the liquid sheet which is of particular interest for understanding the disintegration process. The location of the first perforation was defined as the distance from the nozzle slot to the upper edge of the hole. To eliminate edge effects, which are not present on a conical sheet, only the central 10mm of the flat liquid sheet images was studied. A datum time was chosen, just prior to the emergence of liquid from the slot, with subsequent image times referenced to this datum in 1ms steps until the end of injection. An example of the injection process is illustrated in Figure 2, showing the parallel liquid sheet under an injection pressure of 20 bar. The parallel liquid sheet provided a datum for the subsequent work which focused on divergent liquid sheets. Instabilities induced by the sheet thinning affects of a divergent sheet accelerated the break-up process and showed similar characteristics to a pressure-swirl spray under low pressure conditions.

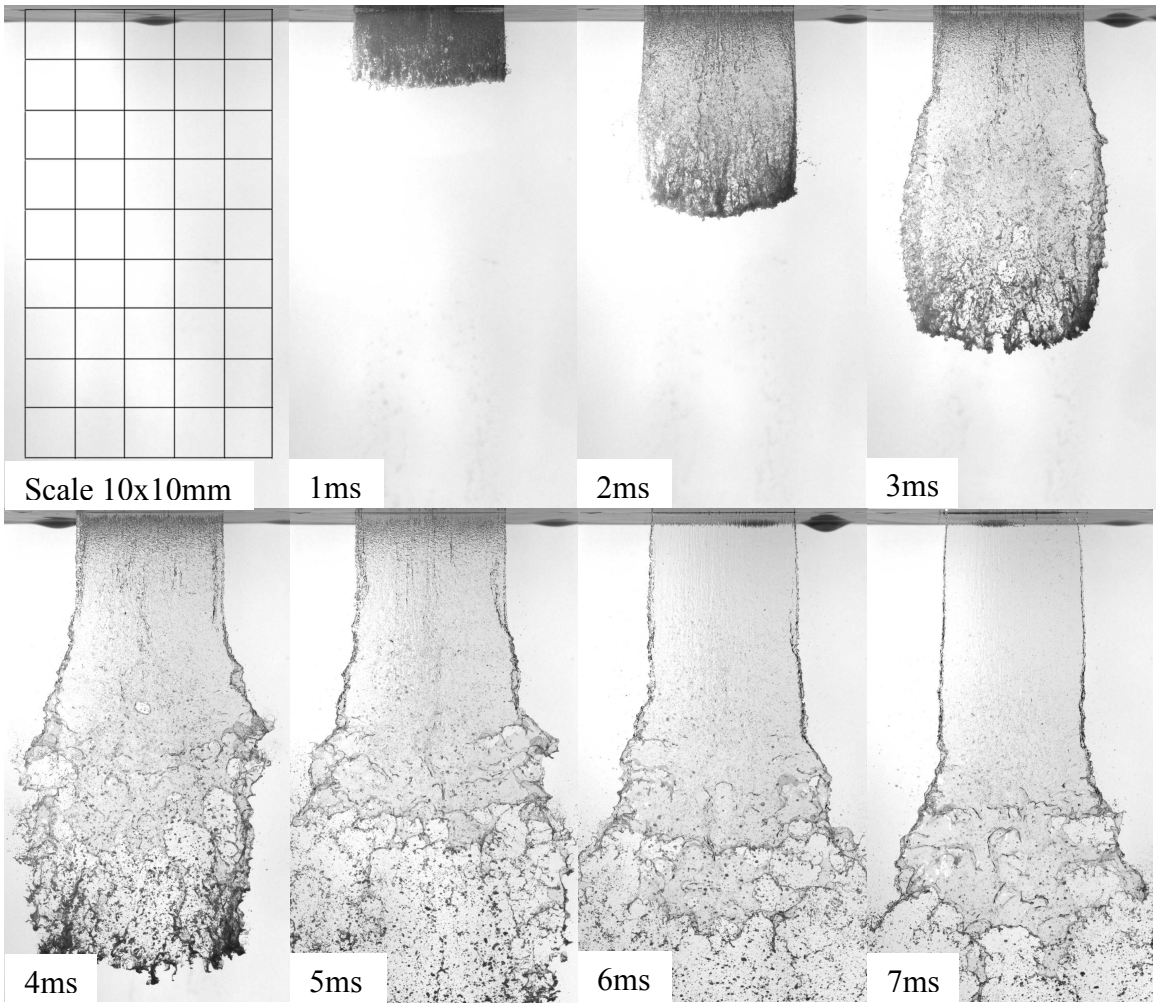

Figure 2. Development of parallel liquid sheet under 20 bar injection pressure in 1ms steps

As the injection pressure is increased sheet stretching is more effective and aerodynamic forces are more influential in the break-up process, Figure 3, affecting the position of perforation onset by as much as 30% at the higher velocities. The non-dimensional perforation onset length with total penetration is a good indication of the break up effectiveness. As the sheet velocity was increased the ratio of perforation on-set length to total penetration rapidly reduced in all cases by 40%. This shows that the leading edge penetration increases at a greater rate than the downstream movement of perforations. As the sheet velocity is increased the break-up region occupies a greater proportion of the spray. With further velocity increases the perforation/penetration ratio would continue its downward trend at an increasing rate as the perforations start to move towards the nozzle orifice, i.e. earlier break up. It is anticipated that the ratio would approach a value close to zero at significantly higher sheet velocities. At these high velocities the penetration would in fact reach a maximum as the leading edge would no longer be continuous, but consist of droplets with less momentum and more aerodynamic drag. The perforations, however, would continue to develop earlier.

One highly important parameter is the liquid sheet thickness at break-up, due to its strong influence on the final droplet size distribution. With knowledge of the perforation onset and the geometry of the liquid sheet it was possible using trigonometry to calculate the sheet thickness at the perforation location, Figure 4. The 20° and 30° divergent liquid sheets follow the same temporal trend; the thickness of the liquid sheet at the perforation onset point decreases throughout the injection cycle, 2-7ms, from 115 to 59µm and 98 to 48µm respectively. This is due to the transient nature of the resulting liquid sheet.

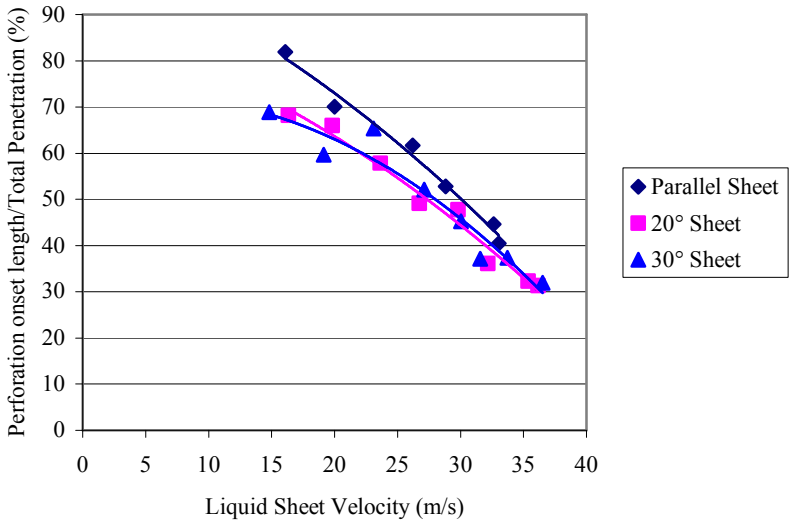

Figure 3. Effect of sheet velocity on perforation development at 3ms after SOI

In the initial stages of injection, 0-2ms, break-up was not observed, however, when perforations do develop, 2ms after SOI , their location is within 26mm of the turbulent leading edge at a point where maximum sheet velocities are present, as will be shown later with the PIV results. This strongly indicates that sheet stretching alone is not responsible for the development of perforations in the sheet; it is a combination of aerodynamic forces, internal turbulence, and sheet thinning, influenced by surface tension and liquid viscosity. As the sheet develops the velocity decreases and the leading edge moves further away from the break-up zone, over 35mm, therefore the influence of aerodynamic and internal turbulent forces decrease respectively. It can therefore be assumed that the sheet thickness, at a time of 5-6ms after SOI, which lie in the range 56 – 88µm are more applicable to the sheet stretching phenomenon of the divergent liquid sheet. After this point the valve has closed and the sheet will start to thin due to a reduction in liquid mass flow.

Comparing the 20° and 30° divergent sheets, Figure 4, there is an estimated sheet thickness variation of 20µm throughout the entire injection. Perforations generally occur at the same distance downstream from the nozzle, but the increased divergence of the 30° sheet leads to a thinner theoretical sheet thickness at the break-up point. At low injection pressures the liquid did not follow the 30° divergence angle so the estimated sheet thickness is lower than expected. The sheet thickness at break-up should be the same for a given injection condition, regardless of divergence angle, however, the position of perforation onset would move towards the nozzle at higher divergent angles.

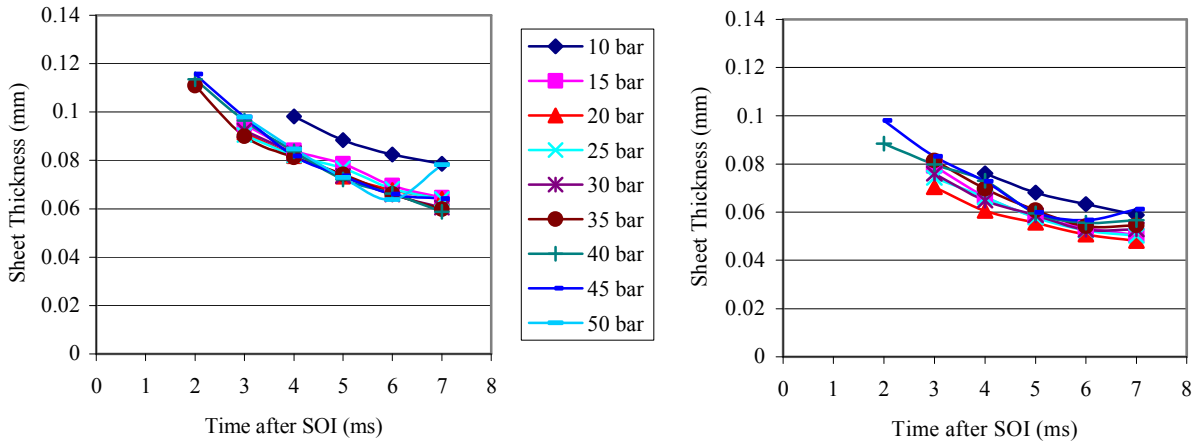

Figure 4. Liquid sheet thickness at perforation on-set for 20° & 30° divergent sheets

Applying PIV along the spray centreline at 1ms intervals to capture the entire injection, produced velocity profiles for the three nozzle configurations; parallel, 20°, and 30° divergent liquid sheets, under 10, 20 and 30 bar injection

pressures [9, 10]. The spray development for all the configurations exhibited similar characteristics with respect to the velocity field, so results from the 20° liquid sheet will be discussed as typical. The temporal injection, or exit velocity, of the liquid sheet is shown in Figure 5a. These velocities do not correlate with theoretical velocities from inviscid theory due to the large pressure drop across the nozzle. The injection pressure was measured inside the cylinder, however, the liquid travels 11mm through the slot prior to emergence. During the initial stages of injection, the first millisecond, high velocities are found at the orifice due to the high fuel line pressure and the small nozzle slit opening of 390µm. Over the period 1 to 3ms the exit velocity rapidly decreases as the slit valve reaches the maximum opening of 1mm, at 2.5ms, causing the largest pressure drop across the valve. Once the valve begins to close the sheet velocity stabilises, between 3 and 4ms, as the drop in line pressure is counteracted by the decreasing nozzle area. This period of relative stability is short-lived and the exiting liquid sheet decelerates further, between 4 and 5ms, as the valve nears closing. For injection pressures 10, 20 and 30 bar estimated liquid mass flow rates drop to 0.0181, 0.0242, and 0.0325kg/s respectively. The valve closes at 5.1ms causing further deceleration of the liquid. Although 5.1ms is the known end of injection, i.e. the valve has just closed, fuel continues to flow for a further 2ms due to a valve-nozzle depth of 11mm. The decreasing liquid sheet axial velocity also indicates that sheet stretching occurs along the spray axis in addition to the lateral stretching of the divergent sheets.

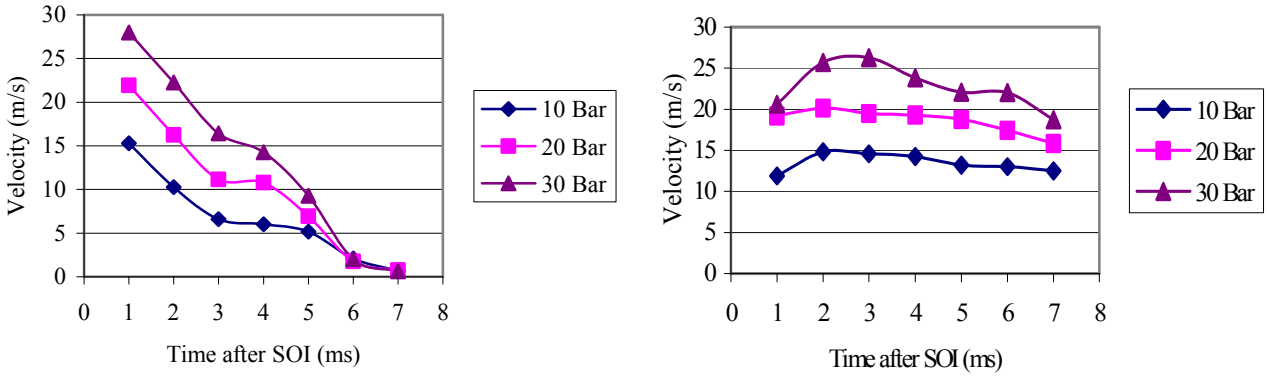

Figure 5. (a) Temporal liquid sheet exit and (b) tip velocity for 20° sheet

The tip of the liquid sheet is less susceptible to velocity fluctuations throughout the injection cycle, Fig. 5b. The acceleration over the first 2ms occurs partly due to the initial presence of static fuel inside the nozzle orifice, hindering the progress of the jet. As the valve starts to open the static fuel is accelerated from rest over a period of 2ms causing the formation of a highly complex and turbulent leading edge flow. This was evident from the simultaneous front and side images, which showed a very dark region up to 5mm thick at the beginning of injection, 1ms, indicating a complex flow structure. The tip velocity subsequently peaks between 2ms and 3ms at the time of maximum valve open. After this point there is a gradual deceleration of the tip, caused by aerodynamic drag on the liquid mass. There is very good correlation between the averaged PIV tip velocity results and the previously measured tip velocities based on temporal penetration. At 20 bar injection pressure there is 2.3% variation and at worst, 30 bar, the correlation is 10.1%.

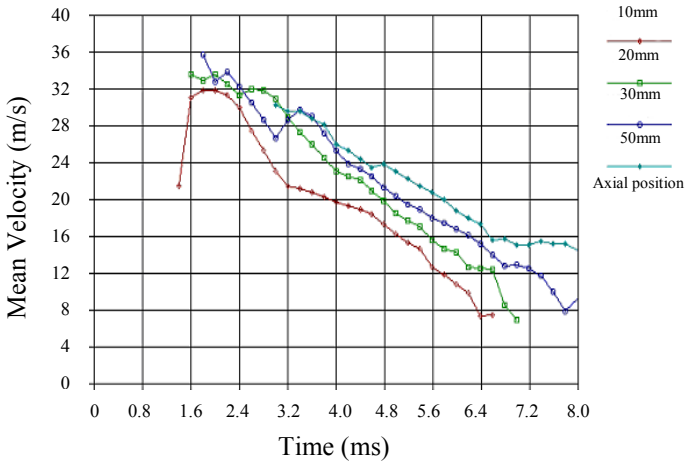

Figure 6. Temporal sheet velocity at 4 axial positons

Laser Doppler Anemometry, LDA, was also applied to the liquid sheet to assess the point wise temporal axial flow velocities for comparison with the PIV data. Only the 20° divergent slot nozzle was investigated under an injection pressure of 30 bar. The location of the peak velocity from the radial scans was used to plot the first 4 axial position velocity profiles as shown in Figure 6. It is assumed that the peak velocity relates to the high momentum of the liquid sheet and represents the sheet velocity.

The LDA velocity data at the 10mm axial position are directly comparable to the exit velocity measured using PIV, Figure 5. Initially there is a sharp decrease in the sheet velocity as the valve opens and passes the fully wide open position, after which the velocity almost stabilises before the valve closing leads to a further deceleration of the liquid sheet. The temporal decay of the liquid sheet velocity is observed at all axial positions. Data for the 75 and 100mm axial positions have not been plotted as the flapping motion of the liquid sheet further downstream made it difficult to locate the point of maximum velocity and hence the spray axis.

Focusing on the time just after the valve fully open position, 3ms, there were several observations from Figure 7, as regards the nature of the liquid sheet and the ability to apply the LDA technique to the flow. The near nozzle velocities have been plotted together with the LDA sample number. The peak velocity at all three locations, 10, 20 and 30mm, occurs 2mm offset from the 'spray axis'. The spray axis was defined as the vertical line through the centre of the nozzle slit. This peak velocity was also accompanied by a drop in sample number at the same locations. This strongly indicates that this was the location of the liquid sheet, which consisted of large fluid elements of high momentum, hence, maximum velocity. The absence of small droplets at this location reduced the sample count, by as much as 40%. There is a large shear layer, up to 2mm, either side of this location as the droplet velocity decreases rapidly towards the spray periphery. It is plausible that the presence of this large shear layer promotes break up from the surface of the liquid sheet, forming smaller droplets, leading to the observed rise in the number of samples. The presence of more droplets at the spray periphery was observed from the spray side imaging. It was also apparent that, due to the nozzle geometry, the liquid sheet did not exit the slit truly in the vertical direction, and hence accounts for the 2mm spray offset in Figures 7, 8, and 9. It is believed that the design of the nozzles causes the spray offset and the opening event has little effect.

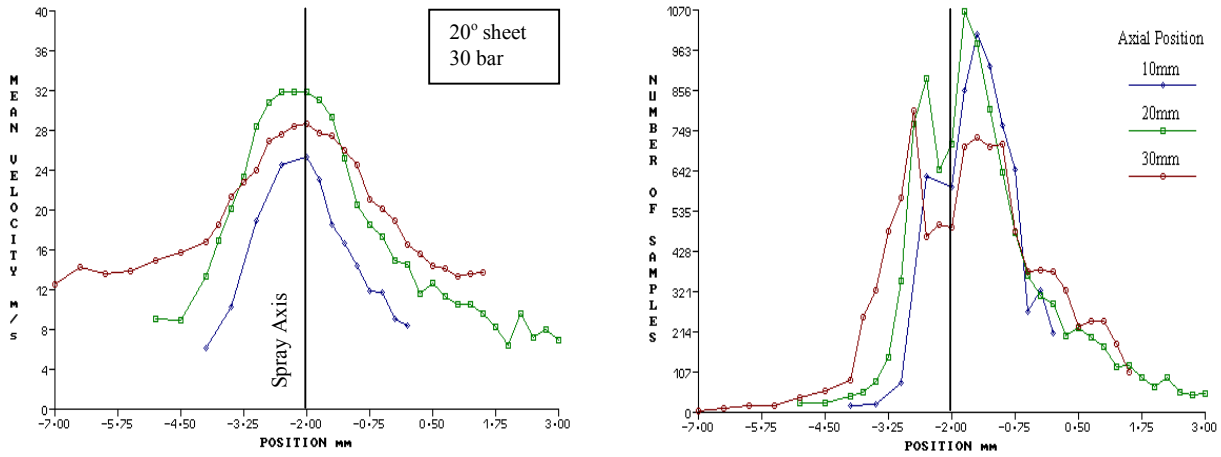

Figure 7. Flow field in near nozzle region at 3ms after SOI

During the course of the investigation it was observed that there was a significant rise in fuel temperature due to the frictional heating of the rotating cylinder, accompanied by a visible change in the sheet break up structure. It was therefore not possible to acquire data for long periods of time. The rotary valve was left to cool down naturally between runs to ensure consistent results were achieved.

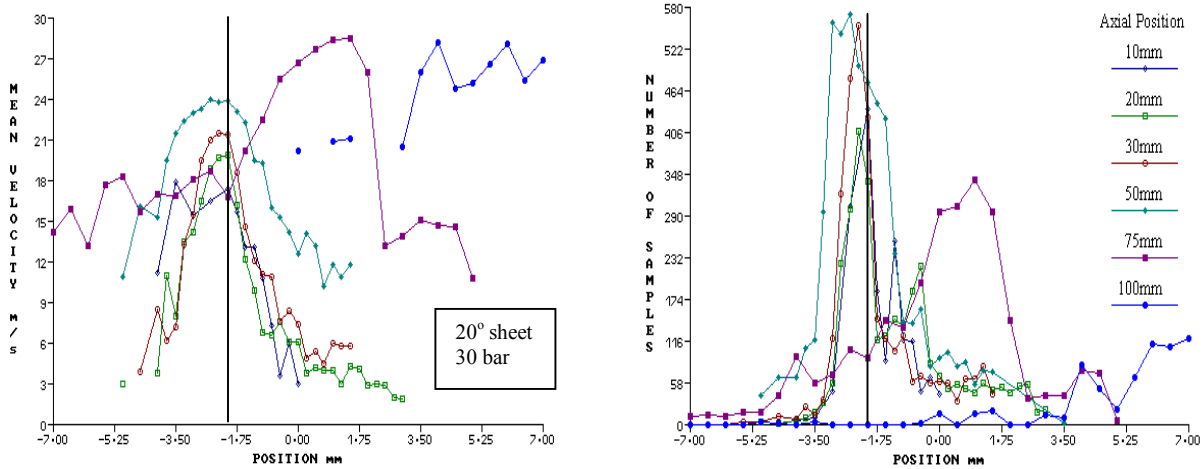

Figure 8. Flow field in near nozzle region at 5ms after SOI

At a later stage in the injection, 5ms, the spray has penetrated further and more data were available at the lower axial positions, as shown in Figure 8. The peak velocities have decreased in the near nozzle region, as indicated by the PIV results, due to the decreasing injection pressure with the closing of the rotary valve. This was coupled with a decrease

in the number of samples as the liquid sheet is decelerating, leading to a possible reduction in droplet formation. The previous sample number reduction in the spray centre at a time of 3ms was not encountered at 5ms as the liquid sheet was more stable in the near nozzle region ensuring higher levels of signal detection through the sheet.

At the 75mm axial location, the velocity profiles change dramatically, with the peak velocity, at 4 and 5ms, moving 2.5mm away from the offset spray axis. Velocity plots for the 20mm and 75mm locations are shown in Figure 9 to allow comparison. It was believed that the offset of the peak velocity, and hence the liquid sheet, was caused by large scale waves, of an approximate wavelength of 40mm.. This sheet 'flapping' motion caused the velocity profile to move, between 4 and 5ms, but once the rotary valve closed there was a flattening of the velocity profile, once again centralised on the vertical axis. After 6ms, the velocity profiles at the downstream positions, of 75 and 100mm, show comparably moderate shear layers with the development of flatter velocity profiles. This was caused by the reduction of injection pressure, i.e. end of injection, and break-up of the liquid sheet into droplets with less momentum.

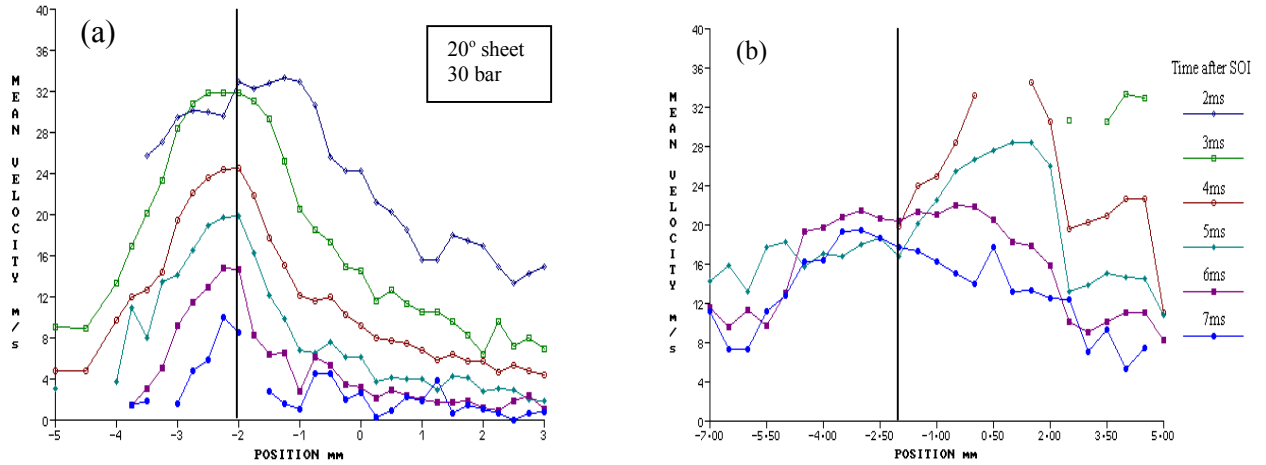

Figure 9. Temporal velocity at (a) 20mm and (b) 75mm

A Phase Doppler Anemometry, PDA, analysis of the spray was also attempted, however, this was problematic due to the nature of the liquid sheet and the poor atomisation. In the near nozzle region there are very few droplets present, as most of the spray consisted of fuel 'elements' that had broken away from the continuous liquid sheet. The few droplets/fuel elements that were measured at the 10mm axial location lay in the size range 5 – 40μm, with the larger droplets located on the spray centre, i.e. significantly smaller than the nozzle width of 150μm. Further downstream, the PDA data rate was still very low due to the presence of irregular shaped liquid elements in the early stages of break up which were rejected by the signal processor. Another potential problem was taking LDA/PDA measurements through the wavy liquid sheet. Relative distortions of the laser beams would invariably move the measurement volume and in severe cases prevent the formation of the measurement volume. In the near nozzle region the traverse distance through the liquid sheet was a maximum of 5mm. Therefore, with a beam separation of only 0.84mm at this point the relative beam positioning would be less susceptible to distortion from any large amplitude surface disturbances. Small disturbances may cause some distortion, however, this could be assumed negligible based on the consistency of the LDA data.

A comparison of the PIV velocity data with the peak LDA velocity data for a particular position and time in the injection cycle, showed significant differences, of up to 30%, with LDA velocities always the greater. The strong velocity gradients across the spray, highlighted by the LDA results, show the importance of correct positioning of the focal plane for PIV analysis. The PIV results were obtained using back illumination and a 55mm macro lens with a 5mm depth of field. Using this illumination method, it was not possible for the PIV to focus on any particular plane and pick out the high velocity gradients across the sheet surface, mainly due to the relatively large depth of field of the lens. This meant that the results obtained using PIV were an average of the flow velocity which accounts for the large difference between LDA and PIV. A more accurate PIV method would involve the use of a laser sheet to illuminate a thin plane through the liquid sheet. However, due to the complex three dimensional dynamics of out-of-plane waves on the transient liquid sheet the alignment of the laser sheet would be challenging.

Further work aims to improve the performance of the rotary valve to allow successful comparisons between a transient flat liquid sheet and a pressure swirl hollow cone GDI spray. The idea of simplifying a 3-dimensional liquid sheet to a 2-D geometry, while replicating the same break up process provides a greater ability to identify causes of break up in the 3-D cone.

4. CONCLUSIONS

To allow the study of transient two-dimensional liquid sheets, the design and development of a unique rotary valve has been undertaken. The rotary valve was configured to produce an injection duration of 5.1ms and allow the study of 3 liquid sheets of typical dimensions 30mm x 0.15mm, in the fuel pressure range 10 – 50 bar. Sheet divergence of 20° and 30° was simulated to promote the sheet stretching effects associated with a GDI pressure-swirl spray.

Assessing the break-up behaviour of the liquid sheet it was observed that the introduction of sheet stretching, by spreading the liquid laterally, affected the position of perforation onset by as much as 30% at the higher velocities. This was expected due to the destabilising effect of the sheet thinning, aiding the break-up process. Estimated sheet thickness at the perforation location based on the sheet geometry were calculated to be in the range 0.05 – 0.1mm.

To assess the flat liquid sheet velocity flow field PIV and LDA were used. The PIV data indicated a large velocity gradient between the nozzle orifice and the spray leading edge, suggesting the presence of axial sheet stretching. The LDA data, collected at various axial positions downstream from the nozzle, showed peak velocities of up to 36m/s on the spray centerline as expected, due to the presence of a liquid sheet/fluid elements of high momentum.

More work is required to gain a complete understanding of the transient behaviour of the flat liquid sheet. Information on perforation development, surface wave structures and sheet thickness at break-up for various liquid sheet geometries can be related to the droplet size distribution further downstream. It is envisaged that the flat sheet data can then be correlated with data obtained from the more complex conical liquid sheets produced by GDI injectors.

5. REFERENCES

1. K. Noma, Y. Iwamoto, N. Murakami, K. Iida, and O. Nakayama, Optimized Gasoline Direct Injection Engine for the European Market, SAE Transactions, SAE 980150, p226-233, 1998.
2. J. Harada, T. Tomita, H. Mizuno, Z. Mashiki, and Y. Ito, Development of Direct Injection Gasoline Engine, SAE Transactions, SAE 970540, p767-776, 1997.
3. K. Heukelbach, S. Jakirlic, R. Nakic and C. Tropea, Influence of Turbulence on the Stability of Liquid Sheets, ILASS-Europe 2002.
4. C. Siegler, A. Lozano, F. Barreras, The Influence of Air Co-Flow Characteristics on the Oscillation of a Liquid Sheet, ILASS-Europe 2002.
5. M. Yamakawa, S. Isshiki, J. Lee, and K. Hishida, 3-D PIV Analysis of Structural Behavior of D.I. Gasoline Spray, SAE 2001-01-3669.
6. P. Broll and P. Walzel, PIV Measurements in Pressure Swirl Atomizers, ILASS-Europe 2001.
7. G. Wigley, M. Goodwin, G. Pitcher, and D. Blondel, Imaging and PDA Analysis of a GDI Spray in the Near Nozzle Region, Applications of Laser Techniques to Fluid Mechanics, Lisbon 2002.
8. M. Goodwin and G. Wigley, A Fundamental Study of Liquid Sheet Breakup and its Relationship to GDI Sprays, ICLASS 2003.
9. M. Goodwin, Transient Liquid Sheets and Their Relationship to GDI Sprays, PhD Thesis, Loughborough University, April 2004.
10. M. Goodwin and G. Wigley, A Study of Transient Liquid Sheets and Their Relationship to GDI Fuel Sprays, International Symposium on Diagnostics and Modelling of Combustion in Internal Combustion Engines, Comodia 2004.